Microcavity morphology optimization

Fahmida Ferdous,[1] Alena A. Demchenko,[2] Sergey P. Vyatchanin,[2] Andrey B. Matsko,[1] and Lute Maleki[1]
[1]*OEwaves Inc., 465 North Halstead Street, Suite 140, Pasadena, California 91107, USA*
[2]*Physics Department, Moscow State University, Moscow 119992, Russia*
(Received 2 April 2014; revised manuscript received 14 July 2014; published 17 September 2014)

High spectral mode density of conventional optical cavities is detrimental to the generation of broad optical frequency combs and to other linear and nonlinear applications. In this work we optimize the morphology of high-Q whispering gallery (WG) and Fabry-Perot (FP) cavities and find a set of parameters that allows treating them, essentially, as single-mode structures, thus removing limitations associated with a high density of cavity mode spectra. We show that both single-mode WGs and single-mode FP cavities have similar physical properties, in spite of their different loss mechanisms. The morphology optimization does not lead to a reduction of quality factors of modes belonging to the basic family. We study the parameter space numerically and find the region where the highest possible Q factor of the cavity modes can be realized while just having a single bound state in the cavity. The value of the Q factor is comparable with that achieved in conventional cavities. The proposed cavity structures will be beneficial for generation of octave spanning coherent frequency combs and will prevent undesirable effects of parametric instability in laser gravitational wave detectors.

DOI: 10.1103/PhysRevA.90.033826 PACS number(s): 42.25.Fx, 42.60.Da, 42.79.Bh

I. INTRODUCTION

An ideal optical cavity can be considered as a single dimensional object with a well-defined "fundamental," nearly equidistant, spectrum. The majority of realistic optical cavities have large spectral density of modes of nearly identical quality (Q) factors and in addition to the fundamental mode family many high-order modes are present in the cavity [1]. This is an undesirable feature for various applications. For instance, when a cavity is used as a linear optical filter, high-order modes result in additional undesirable frequency-dependent rejection or transmission of a signal of interest, reducing the efficacy of the filter [2–4]. High-order modes also lead to mode competition in lasers [5] and tend to cause unwanted nonlinear instabilities in optical sensors and oscillators. The difference in the environmental sensitivity of the fundamental and high-order modes adds complexity to the system because it becomes difficult to predict the spectrum of a cavity, especially a monolithic one with a reasonably large geometrical size, as a minute change of the ambient temperature leads to a change in the cavity spectrum.

Very recently it was found that the high spectral density of modes in whispering gallery mode (WGM) microcavities significantly impacts generation of Kerr optical frequency combs [6–13]. High mode density results in mode interaction, mediated by the imperfect shape of the cavity, and modifies the phase-matching conditions responsible for comb excitation. This process results in an unexpected soft excitation regime of frequency combs in microcavities with nominally normal group velocity dispersion (GVD) [6,12]. The same process limits the growth of the frequency comb in cavities characterized with anomalous GVD [8]. It is essential to create a nonlinear cavity free of mode interaction to generate ultrabroad optical frequency combs on a chip.

Seemingly independent problems also arise on a macroscale due to a high density of modes in a Fabry-Perot (FP) cavity. It has been found that a large mode density of a conventional FP resonator results in optomechanical parametric instability in laser gravitational wave detectors [14–18]. This instability restricts the optical power circulating in the detectors and limits the ultimate sensitivity of the measurements. The problem can be solved by reducing the Q factors of the auxiliary optical modes that lead to instability.

The density of a cavity frequency spectrum can be reduced rather significantly by changing the cavity morphology. One can get rid of the unwanted modes by properly shaping mirrors of a FP [19–21] or the circumference of a WGM cavity [24,25]. The method draws from quantum mechanics permitting existence of a potential well with a single bound state [26]. Both FP and WGM cavities can be approximated by a time-independent Schrödinger equation with a potential term determined by their morphology. It is possible to create a single-mode-family cavity since it is possible to select a potential having only one bound state.

The method raises a fundamental question related to the lifetime limitation of the bound state. The Schrödinger equation model does not tell much about the Q factor of cavity modes. The lifetime of the bound state is expected to be short due to various effects not taken into consideration. For example, diffraction loss becomes important if the potential is too shallow and the system has finite overall dimensions comparable with the size of the well. Increasing the well depth results in increased lifetime, but it also leads to eventual confinement of higher-order modes. In addition, the lifetime of light circulating in unbounded modes can still be significant, so the "single-mode" feature becomes compromised. The question arises if it is practically possible to create a single-mode cavity with high-enough Q factor; reduction of Q factor below a certain limit makes the cavity useless for many applications. It is also important to know the maximal ratio of the bounded and unbounded modes for a cavity of a finite size. Finally, it would be interesting if the Q factor depends on the type of the cavity, since different types of cavities have different loss mechanisms.

Loss in FP cavities having both bound and unbound modes has been evaluated previously [21]. It was found that the bounded modes have Q factors that increase exponentially

with the mirror diameter, while the Q factors of the unbounded modes follow a power law dependence on the diameter. Thus, it is possible to achieve an infinite ratio of the Q factors for infinite mirrors. That study does not evaluate limitations imposed by the finite resonator size when the mirror shape is considered as a free parameter.

An analytical study of finite-size single-mode cavities is rather challenging. In this paper we investigate numerically a method for reduction of the complexity of the cavity frequency spectrum by optimizing the cavity morphology, using two distinct examples of optical cavities: WGM and FP. We show that very high-Q single-mode-family cavities of both kinds are practically feasible. For the sake of clarity we select cavities with 10 GHz free spectral range (FSR) excited with 1.55-μm-wavelength light. The transverse dimension of the cavities does not exceed 0.1 cm. We confirm that it is possible to make both single-mode-family FP and single-mode-family WGM cavities by engineering their morphology and find the lifetime of light circulating within the bound modes. The single-mode regime is achieved for a limited range of geometrical parameters of the cavities.

While the simulations are performed for microcavities, the conclusions hold for cavities of any size, including kilometer-scale laser gravitational wave detectors. In what follows it is shown that the problem we solve can be parameterized in such a way that the single-mode FP cavity is mathematically scaled to any desirable size. It means that a kilometer-size cavity could have properties similar to those of a microcavity. A similar scalability feature was previously predicted for single-mode WGM cavities [24].

We found that the Q-factor value of the single-mode FP cavity is comparable with the value of the diffraction-limited Q factor of a FP cavity with ideal spherical mirrors, when both cavities are matched in length. For the given dimensions the Q factor of the basic mode family is $Q = 1.1 \times 10^9$, according to our numerical simulations. We found that Q factors of the single-mode FP cavity can exceed this number and the maximum ratio of the Q factors of the bound and the highest Q unbound mode exceeds 1000.

The Q factor is not diffraction limited for a large (a few millimeters in diameter) conventional overmoded WGM cavity. Fundamental radiative loss is the only unavoidable, and usually negligible, loss mechanism in the cavity. It is shown theoretically that for a water droplet having a radius of 50 μm localized in air the radiation-limited quality factor is 10^{73} at wavelength 0.6 μm [22,23]. The best practically achieved number for a quality factor for a conventional WGM resonator exceeds $Q = 10^{11}$ [27], limited by the absorption of the material. We found that Q factors of the single-mode WGM cavity can exceed $Q = 10^{10}$ and the maximum ratio of the Q factors of the bound and the highest Q unbound modes is approximately 1000, similar to that of the single-mode FP cavity. These results imply that it is practical to make these kinds of devices suitable for various applications.

The paper is organized as follows. In Sec. II we discuss limitations of Q factor values for single-mode WGM cavities. A study of Q factors in single-mode FP cavities is presented in Sec. III. Similarities and differences between behaviors of WGM and FP single-mode cavities is discussed in Sec. IV. Section V concludes the paper.

II. SINGLE-MODE WGM RESONATORS

In this section we present a simple analytical model to show the possibility of existence of a single-mode WGM resonator and find a range of parameters where single-mode operation takes place [24].

A. Analytical description of a single-mode WGM cavity

We start from the scalar wave equation

$$\nabla \times (\nabla \times \mathbf{E}) - k^2 n^2 \mathbf{E} = 0, \tag{1}$$

where $k = \omega/c$ is the wave number, n is the index of refraction of the resonator host material, $\mathbf{E}$ is the electric field of the mode. For the sake of simplicity we neglect material loss and consider the TE mode family.

Changing variables in Eq. (1) as

$$E = \Psi e^{\pm il\phi} \frac{1}{\sqrt{r}}, \tag{2}$$

where $l \approx kna \gg 1$ is angular momentum number of a WGM, and assuming that the resonator radius changes as $R = a + A(z)[a \gg A(z)]$, we arrive at

$$\frac{\partial^2 \Psi}{\partial r^2} + \frac{\partial^2 \Psi}{\partial z^2} + \left\{ k^2 n^2 \left[1 + 2\frac{A(z)}{a} \right] - \frac{l^2}{r^2} \right\} \Psi = 0. \tag{3}$$

Example of such a resonator is shown at Fig. 1(a). Equation (3) shows that geometrical change of the resonator radius is equivalent to the spatially dependent increase of the refractive index of the resonator host material.

Introducing $\Psi = \Psi_r \Psi_z$, we separate variables

$$-\frac{\partial^2 \Psi_z}{\partial z^2} - 2k^2 n^2 \frac{A(z)}{a} \Psi_z = k_z^2 \Psi_z, \tag{4}$$

$$\frac{\partial^2 \Psi_r}{\partial r^2} + \left(k^2 n^2 - k_z^2 - \frac{l^2}{r^2} \right) \Psi_r = 0, \tag{5}$$

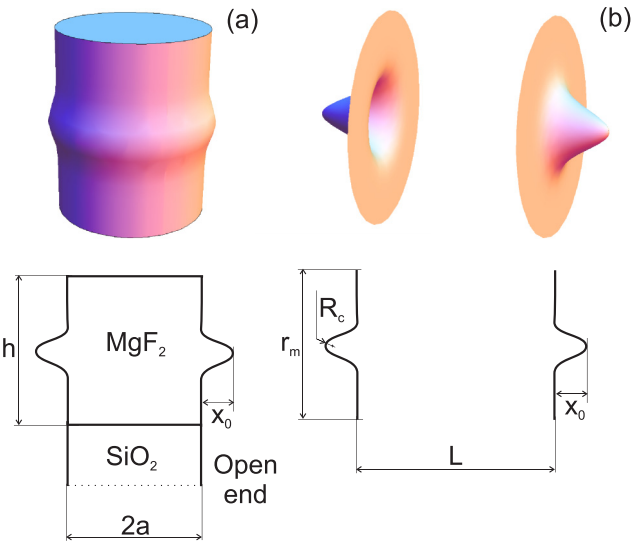

FIG. 1. (Color online) Morphologies of the studied cavities: (a) single-mode WGM cavity; (b) single-mode FP cavity.

where k_z^2 is the separation parameter. Equation (4) is equivalent to a time-independent Schrödinger equation describing the motion of a particle in a potential well.

The derivation has two crucial assumptions so far: One is exchange of the term $-l^2/r^2$ with term $-l^2/r^2 + 2A(z)l^2/a^3$ to reflect change of the resonator radius, and the other is the assumption that variables can be separated in Eq. (3). These assumptions are valid if we consider high-order WGMs with fields localized in the vicinity of the surface of the resonator. Numerical simulations presented in what follows validate the derivation steps.

To show that the cavity can have only one localized TE mode, we further simplify the problem and assume that $A(z) = x_0$ if $p/2 \geqslant z \geqslant -p/2$. If x_0 is large enough we get the standard eigenvalues for the low-order modes of the well:

$$k_{z,j} \simeq \frac{\pi j}{p}, \quad j = 1,2,3,\ldots. \tag{6}$$

The eigenvalues for the localized cavity modes can be estimated in this case as

$$k^2 n^2 \simeq \frac{1}{(a+x_0)^2}\left[l + \alpha_q\left(\frac{l}{2}\right)^{1/3}\right]^2 + \frac{\pi^2 j^2}{p^2}, \tag{7}$$

where α_q is the qth root of the Airy function, $\mathrm{Ai}(-r)$, which is equal to 2.338, 4.088, and 5.521 for $q = 1,2,3$, respectively.

The wave vector of the unlocalized modes (continuum) of the cavity is simply

$$k_c^2 n^2 \simeq \frac{1}{a^2}\left[l + \alpha_q\left(\frac{l}{2}\right)^{1/3}\right]^2. \tag{8}$$

The condition of localization of the jth mode is $k_c > k$ or

$$\sqrt{\frac{2x_0}{a}}\frac{2n}{\lambda} > \frac{j}{p}. \tag{9}$$

Only one mode is supported by the resonator if

$$1 > \sqrt{\frac{x_0}{a}}\frac{2np}{\lambda} > \frac{1}{2}. \tag{10}$$

Equation (10) shows that there is a region of parameters for which the WGM cavity spectrum has a single-mode family in each polarization. As the derivation of the equation has many strong assumptions the predicted range of the parameters gives only order-of-magnitude accuracy. In addition, it does not give any clue about the quality factor of the cavity modes. In what follows we present results of numerical simulations performed for a particular WGM cavity that validates the analytical calculation and also describes the behavior of the Q factor as function of parameter x_0.

B. Numerical modeling of a single-mode WGM cavity

In this section we numerically study a WGM cavity with morphology illustrated by Fig. 1(a). A MgF_2 cavity with thickness $h = 60$ μm and radius $a = 0.35$ cm is considered. The cavity has 10 GHz FSR [$c/(2\pi an)$, $n_{WGM} = 1.36$ is the refractive index of the material, c is the speed of light in the vacuum]. The rim of the cavity has a Gaussian geometric shape characterized with 10 μm full width at half maximum (FWHM) and a variable height,

$$A(z) = x_0 \exp\left[-\left(\frac{z - h/2}{p}\right)^2\right], \tag{11}$$

where $p^2 = 36.1$ μm^2 corresponds to the FWHM selection. The Gaussian profile is selected since this kind of profile has been demonstrated experimentally [25]. The considered example is rather general since the value of FWHM is not essential to create a single-mode WGM cavity and the results of the simulations do not fundamentally change for different FWHM values. Single-mode operation is still observed at different values of x_0, as indicated by Eq. (10).

Using x_0 as a free parameter we find the lifetime of the cavity modes and identify the single-mode operation regime. Analytical theory gives reasonably good approximation of the dynamic range of the single-mode operation of the cavity. Substituting the effective value of resonator width [we select it to be equal to FWHM of the Gaussian $2(\ln 2)^{1/2}p = 10$ μm] into Eq. (10), we find that single-mode operation is possible for 8 μm $\geqslant x_0 \geqslant 2$ μm. In what follows we show that for the given realistic model of the resonator single-mode operation is possible for practically the same values of x_0. This result is not obvious, though, since the analytical model is rather different from the structure studied numerically.

In accordance with the analytical model of a single-mode WGM cavity, there is a limited region of protrusion heights, x_0, when only a single bound mode family exists. The analytical model, though, requires the cavity thickness, h, to be infinite. Hence, conclusions of the analytical model are not directly applicable to the case of a finite-size cavity. A symmetric protrusion does not result in a change of the number of bound modes and their Q factors in such a cavity. All the modes have nearly identical (high) Q factors and simply change their spatial distribution as compared with an unperturbed stand-alone multimode cylindrical cavity. Similarly, the core of a single-mode fiber, stripped off its cladding, becomes a multimode fiber. Thus, in a cavity structure, the Q factors of unwanted modes may be reduced similarly to the cladding of single-mode optical fibers.

To address this problem we place the WGM cavity on a SiO_2 substrate. The substrate introduces additional attenuation to the modes since its refractive index, $n_s = 1.44$, is larger than that of the cavity host material. We equip the substrate with antireflection coating to ensure that the light entering the substrate does not return to the WGMs.

The presence of a higher-index substrate is important from both theoretical and practical points of view. From a theoretical perspective, placing antireflection coating directly at the bottom of the cavity results in an infinite continuation of the cavity body. It leads to an increase of the Q factor of the localized modes independent of the degree of their localization. This is undesirable since the numerical procedure does not allow reliable simulations of very high Q factors. From an experimental perspective, cavities of finite size have to be mounted on a substrate to facilitate single-mode operation. The substrate increases loss of unbounded modes much stronger if compared with loss increase of the bound modes. Our numerical model describes exactly this case.

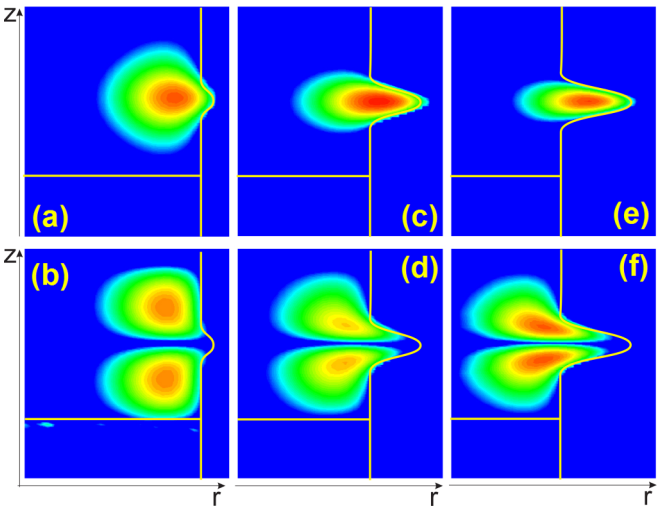

FIG. 2. (Color online) Spatial profile of the field intensity for the fundamental and the first dipole WGMs for different height of the protrusion: (a),(b) $x_0 = 2$ μm; (c),(d) $x_0 = 8$ μm; and (e),(f) $x_0 = 11$ μm. The intensity is illustrated by color density.

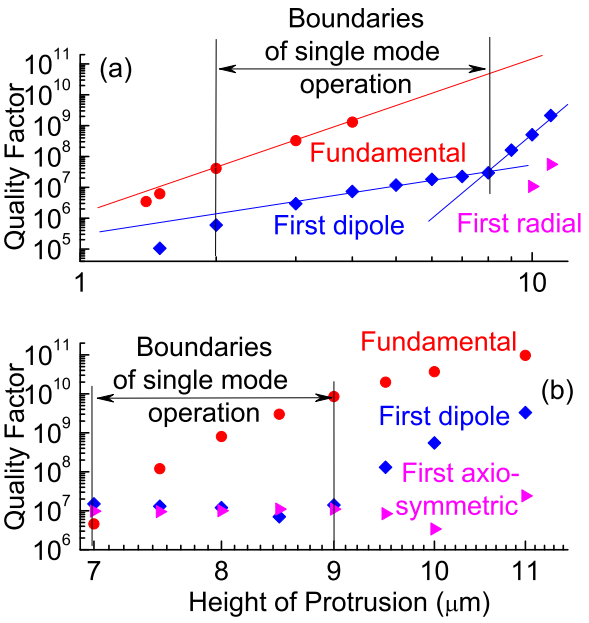

FIG. 3. (Color online) Dependence of the Q factors of the fundamental and the first dipole as well as the first higher-order radial modes [quantization by q number; see Eq. (7)] on the protrusion height for a WGM cavity (a) and a FP cavity (b). The numerical model is not accurate enough to predict Q factors below 10^6 and above 10^{10}.

Our approach utilizes COMSOL software to solve the Helmholtz equation using Galerkin's method of weighted residuals [28]. The three-dimensional (3D) problem is reduced to a 2D problem because of azimuthal symmetry of the cavity modes. Perfectly matched layers (PMLs) [29] are used to simulate power loss of the modes originating from the mounting substrate. The layers block unwanted reflections from the edges of the substrate taken into consideration in the code. Because of the loss introduced by the PML, the frequencies of the modes (ν_0) become complex and the Q factor is calculated as $Q = \mathrm{Re}\ \nu_0/(2\mathrm{Im}\ \nu_0)$.

Results of the simulation (Fig. 2) show that light escapes to the higher-index substrate from both fundamental and first-order dipole modes if the height of protrusion is small enough. The field leaving the WGM is transferred to a Bessel beam freely propagating in the substrate [30,31]. Hence, the substrate can be considered as an ideal coupler for generation of Bessel beams out of the resonator.

The energy exchange efficiency reduces with the increase of the protrusion height. It also depends on the mode order. There are two critical regimes corresponding to no-bound states for $x_0 = 0$ and a nearly infinite number of high-Q bound states for $x_0 p^2 \gg a\lambda^2$ [24]. The consequence of the protrusion increase is clearly seen in Fig. 3(a), showing dependence of the Q factor of the fundamental and lowest-order dipole WGMs. No modes are confined for small x_0. The first mode becomes trapped as x_0 reaches a certain threshold value, equal to 2 μm for the selected model. Its Q factor grows exponentially; however, it is still finite. The Q factor of the first dipole mode, on the other hand, barely changes. As the protrusion reaches another threshold point, $x_0 \simeq 8$ μm, the Q factor of the second mode starts to grow as well, which means that the mode becomes bound. It is worth noting here that the Q factors of unbound modes increase with protrusion height increase. However, the rate of increase is significantly different than the rate of increase of the bound mode.

Our method of Q evaluation does not allow evaluating Q's exceeding several billion and undershooting several hundred thousands. The simulations of the high-Q modes become inaccurate when the imaginary part of the eigenvalue becomes comparable with the simulation error. The simulations of low-Q modes are limited in accuracy because the modes overlap too much in frequency space and because an equivalent Q of a piece of a material that has no mode confinement is still finite and comparably large. For instance, the equivalent Q factor of a piece of a material having length corresponding to the WGM cavity length is approximately $2\pi^2 an/\lambda$, which is 6×10^4 for the cavity of the given size. The numerical simulation gives wrong answers if the actual Q factor is close to this value as the code looks for confined modes. The reliable simulation results are achieved for a cavity that supports more than ten round trips, which pushes the minimal simulated Q factor to 10^6.

The numerical simulation confirms the prediction of the simplified analytical theory showing that there exists a certain range of protrusion heights where the cavity can be treated as single mode [24]. It also shows that the maximum ratio of the Q factors of the bound and unbound modes is reached just before the second-lowest-order mode becomes bound. For the given cavity geometry the ratio is approximately equal to a 1000. The Q factor of the fundamental mode reaches its maximum at the same point. We find the maximum using interpolation. The simulation does not answer to the question related to the optimal cavity morphology to reach the highest possible Q factor under the condition of the largest Q-factor difference.

C. Variation of WGM cavity shapes

We have shown in a previous section that a high-Q WGM cavity with Gaussian shape of protrusion can be created. The

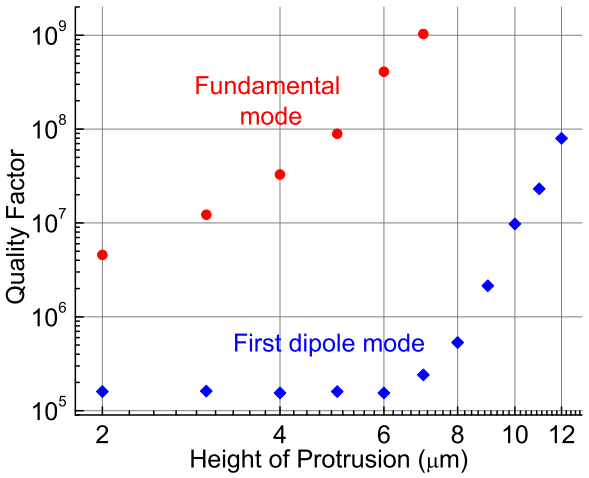

FIG. 4. (Color online) Dependence of the Q factors of fundamental and first dipole mode versus the protrusion height. The simulation is performed for a WGM cavity formed by a protrusion with a square cross section with 10 μm width. The Q factor of the modes drops below 10^6 for height less than 1.5 μm.

Gaussian shape corresponds to the shape that can be produced experimentally [25]. In this section we explore variations of the problem and solve for the case of a protrusion having a square cross section, as was discussed in Sec. II A and also study dependence of a Q factor on the thickness of the cavity, h, for the case of a Gaussian profile of the protrusion.

Results of simulation of Q factors of the fundamental and dipole modes of a WGM cavity formed by a protrusion with a square cross section is shown in Fig. 4. We found that the cavity operates in the single-mode regime if the protrusion height stays within 7 μm $\geqslant x_0 \geqslant$ 2 μm. Those boundaries are relatively similar to the boundaries we found for the Gaussian-shaped protrusion having 10 μm FWHM. This observation gives us grounds to say that the single-mode regime of

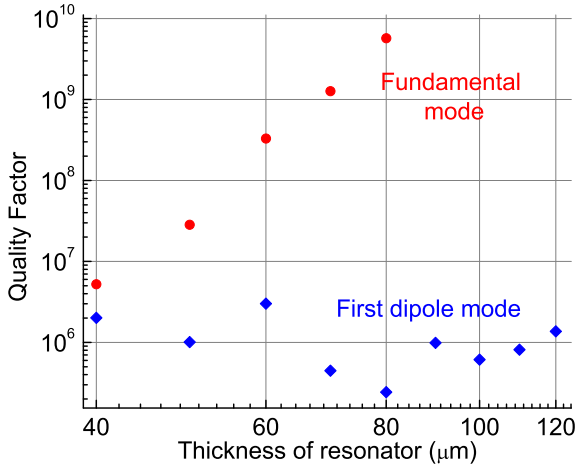

FIG. 5. (Color online) Variation of the Q factor of the basic and first dipole modes of a single-mode WGM cavity with Gaussian shape versus thickness of the cavity, h. The Gaussian is characterized with $x_0 = 3$ μm and 10 μm FWHM.

WGM cavities does not depend strongly on the protrusion morphology. The height and width of the protrusion matter.

An important question is related to the dependence of the Q factor of the WGM cavity on its thickness. The smaller the thickness, the higher is the overlap of the field localized in the cavity mode with the higher-index substrate and the smaller is the Q factor of the mode. We performed a simulation and confirmed this intuitive prediction for the fundamental mode (Fig. 5). Interestingly, the Q factor of the unbound dipole mode did not change much. It means that for selected parameters the dipole mode is strongly delocalized. This also means that for the case of delocalized modes it is possible to increase the ratio of Q factors of the basic and high-order modes beyond the factor of 1000 we found for the resonator with 60 μm thickness.

III. SINGLE-MODE FP CAVITIES

It is not obvious if the FP cavity has properties similar to those of the WGM resonator, because the Q factor of modes of the FP cavity itself is limited due to the diffraction loss, while the WGM Q factor is practically infinite for an isolated cavity. However, both WGM and FP cavities can be described in a similar manner if the Born-Oppenheimer method, instead of paraxial approximation, is used to solve the Helmholtz equation (compare [24] and [32]). The Born-Oppenheimer approach works in the case of the nearly confocal FP cavity

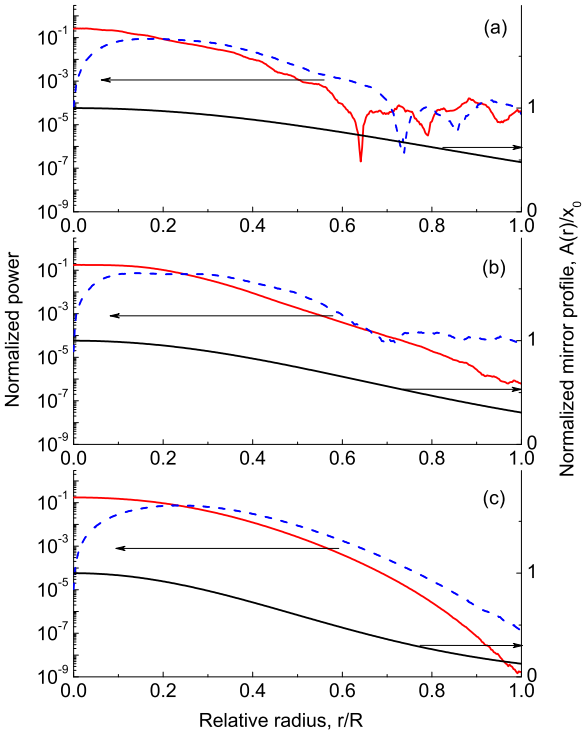

FIG. 6. (Color online) Spatial profile of the FP cavity mirrors and the field intensity for the fundamental (red solid lines) and the first dipole (blue dashed lines) modes for different heights of the mirrors: (a) $x_0 = 5$ μm, (b) $x_0 = 8$ μm, and (c) $x_0 = 14$ μm. The intensity distribution of poorly confined modes have irregular spatial structure resulting from diffraction at the mirror edge. The arrows are used to directly show which scale (left or right) has to be used with each particular curve presented on the picture.

considered here (doubled curvature radius R_c is about FP cavity length L, i.e., $2R_c \simeq L$). Since this approach results in a 2D Schrödinger equation and also allows studying different mirror shapes, we conclude that it is possible to create a single-mode FP cavity if we use the proper mirror profile [see Eq. (31)] and adjust its height parameter (x_0). Our numerical simulation in paraxial approximation confirms this conclusion; see results shown in Figs. 6 and 3(b). The FP cavity can be made with a high-Q single-mode family. For simplicity, we assume below that mirrors of FP cavity are identical and are cylindrically symmetric.

In this section we present an analytical model, following [32], to show the possibility of the existence of a single-mode FP resonator and find a range of parameters where the single-mode operation takes place. We also validate the model and prove existence of high-Q single-mode FP cavities via numerical simulation based on a Fresnel integral equations approach.

A. Analytical description of a single-mode FP cavity

We start from Eq. (1) and rewrite it as

$$\frac{\partial^2\Psi}{\partial z^2} + \Delta_\perp\Psi + k^2\Psi = 0, \tag{12}$$

where z is directed along the cavity axis. The boundary conditions are $\Psi(r,z = L/2 + \tilde{A}(r)) = \Psi(r,z = -L/2 - \tilde{A}(r)) = 0$, where $\tilde{A}(r)$ is mirror profile and r is radial distance from z axis.

The Born-Oppenheimer approach is based on the ansatz $\Psi = \Psi_r(r)\Psi_z(z;r)$, where dependence of $\Psi_z(z;r)$ on radial components can be neglected in the adiabatic approximation. Separating variables we arrive at the equation

$$\frac{\partial^2\Psi_z}{\partial z^2} + k_z^2\Psi_z = 0. \tag{13}$$

This equation has to be supplied with boundary conditions $\Psi_z(r,z = L/2 + \tilde{A}(r)) = \Psi_z(r,z = -L/2 - \tilde{A}(r)) = 0$. The solution of Eq. (13) with the boundary conditions is

$$\Psi_z(z;r) = \cos k_z z, \quad k_z = \pm\frac{1}{L/2 + \tilde{A}(r)}\left(\frac{\pi}{2} + \pi l\right), \tag{14}$$

where l is an integer number.

Equation for $\Psi_r(r)$ can be presented in the form

$$\Delta_\perp\Psi_r + \left[k^2 - k_z^2(r)\right]\Psi_r = 0. \tag{15}$$

Assuming $L/2 \gg \tilde{A}(r)$ we rewrite Eq. (15) as

$$\Delta_\perp\Psi_r + \left\{k^2 - k_0^2\left[1 - \frac{4\tilde{A}(r)}{L}\right]\right\}\Psi_r = 0, \tag{16}$$

$$k_0 \equiv \frac{2\pi\left(l + \frac{1}{2}\right)}{L}. \tag{17}$$

Changing variables in Eq. (15) as

$$\Psi_r = \tilde{\Psi}_r e^{\pm i(m+1/2)\phi}\frac{1}{\sqrt{r}}, \tag{18}$$

we arrive at

$$\frac{\partial^2\tilde{\Psi}_r}{\partial r^2} + \left\{k^2 - k_0^2\left[1 - \frac{4\tilde{A}(r)}{L}\right] - \frac{m(m+1)}{r^2}\right\}\tilde{\Psi}_r = 0. \tag{19}$$

Introducing

$$k^2 = k_0^2 + \tilde{k}^2, \tag{20}$$

where $k_0 \gg \tilde{k}$, we transform Eq. (19) to

$$\frac{\partial^2\tilde{\Psi}_r}{\partial r^2} + \left[\tilde{k}^2 + \frac{4\tilde{A}(r)}{L}k_0^2 - \frac{m(m+1)}{r^2}\right]\tilde{\Psi}_r = 0. \tag{21}$$

For a spherical mirror $\tilde{A}(r) \approx -r^2/(2R_c)$, so Eq. (21) becomes an equation for a harmonic oscillator

$$\frac{\partial^2\tilde{\Psi}_r}{\partial r^2} + \left[\tilde{k}^2 - \frac{2r^2}{R_c L}k_0^2 - \frac{m(m+1)}{r^2}\right]\tilde{\Psi}_r = 0, \tag{22}$$

which has eigenvalues $\tilde{k}$ so that for the whole resonator we get

$$k = \frac{2\pi(l + 1/2)}{L} + \frac{4}{\sqrt{LR_c}}(2q + |m| + 1), \tag{23}$$

where q is the radial quantization number for the modes. We assume that the height of the mirrors is limited by protrusion X_0, which for profile (31) discussed below is equal to

$$X_0 = x_0\left(1 - \exp\left[-\frac{r_m^2}{2R_c x_0}\right]\right). \tag{24}$$

Now we find that the modes become bound if

$$k = \frac{2\pi(l + 1/2)}{L} + \frac{4}{\sqrt{LR_c}}(2q + |m| + 1) < \frac{2\pi(l + 1/2)}{L - 2X_0}, \tag{25}$$

which shows that single-mode operation of the FP cavity becomes feasible for

$$1 \geqslant \frac{\pi X_0}{2\lambda}\sqrt{\frac{R_c}{L}} \geqslant \frac{1}{2}. \tag{26}$$

We see that condition (26) is similar to condition (10) for WGM cavity, including the fact that it predicts only an approximate range of parameters for single-mode operation. Also, it does not give any estimates of Q factors of modes. For these reasons, in the next section we present additionally numerical calculations of modes based on the Fresnel integral approach.

B. Fresnel integral equation approach

We start from the same scalar wave equation (1) as for WGM resonators. However, as we are interested in eigenmodes, it is convenient to use an equivalent formulation of problem through Fresnel integral equations [33,34],

$$\int G(\vec{x}_1,\vec{x}_2)\Psi_2(\vec{x}_2)\,d\vec{x}_2 = \xi\Psi_1(\vec{x}_1), \tag{27a}$$

$$\int G(\vec{x}_1,\vec{x}_2)\Psi_1(\vec{x}_1)\,d\vec{x}_1 = \xi\Psi_2(\vec{x}_2), \tag{27b}$$

$$G(\vec{x}_1,\vec{x}_2) = -\frac{i}{2\pi}\exp\left\{i\left[\frac{|\vec{x}_1 - \vec{x}_2|^2}{2} - y_1(\vec{x}_1) - y_2(\vec{x}_2)\right]\right\}, \tag{27c}$$

where Ψ_1 and Ψ_2 stand for complex field amplitudes at the surface of mirrors, $G(x_1,x_2)$ is the kernel, $d\vec{x}_{1,2} = x_{1,2}dx_{1,2}d\phi_{1,2}$, and ξ is eigenvalue. We use a polar coordinate system with dimensionless coordinates x_1, x_2, which relates to

physical radial coordinate r (dimensional) as $x_{1,2} = r_{1,2}\sqrt{k/L}$, $k = 2\pi/\lambda$ is the wave number, and L is FP cavity length. Dimensionless functions

$$y_1(\vec{x}_1) = kh_1(\vec{x}_1), \quad y_2(\vec{x}_2) = kh_2(\vec{x}_2), \tag{28}$$

describe the mirror profile; the physical profile $h_{1,2}$ of mirrors (dimensional) is a deviation from the mirror plane which depends on corresponding coordinates $\vec{x}_1$, $\vec{x}_2$.

For a FP cavity with two identical and axiosymmetric mirrors, functions Ψ_1 and Ψ_2 should be equal to each other. We perform integration over azimuthal angle and reduce set (27) to single equation which has different kernels for axiosymmetric, dipolar (and so on) modes [33,34],

$$\int g(x_1,x_2)\Psi_1(\vec{x}_2)\,x_2 dx_2 = \xi\Psi_1(x_1), \tag{29a}$$

$$g(\vec{x}_1,x_2) = -i^{\ell+1}J_\ell(x_1x_2)\exp\left\{i\left[\frac{x_1^2+x_2^2}{2} - y_1(x_1) - y_2(x_2)\right]\right\}, \tag{29b}$$

where J_ℓ is a Bessel function of the first kind and ℓ is the angular index ($\ell = 0$ for axisymmetric modes, $\ell = 1$ for dipole modes and so on).

The solution of set (29) provides field distribution Ψ_1 on each mirror, where the absolute value of eigenvalue ξ gives the value of round-trip diffraction loss $\mathcal{L} = 1 - |\xi|^2$.

C. Numerical modeling of a single-mode FP cavity

The reasoning related to the possibility of creation of a single-mode-family cavity seems to be rather general and applicable to any kind of cavity. To verify this intuitive conclusion we consider a FP cavity shaped as shown in Fig. 1(b) with operational wavelength λ, length L, radius of curvature R_c, and radius of mirrors r_m,

$$\lambda = 1.5\ \mu\text{m}, \quad L = 1.5\ \text{cm}, \tag{30a}$$

$$R_c = 0.78\ \text{cm}, \quad r_m = 0.325\ \text{mm}, \tag{30b}$$

$$\rho = \frac{R_c}{L} = 0.52, \quad a = r_m\sqrt{kL} = 5.43, \tag{30c}$$

where ρ is dimensionless curvature radius and a is dimensionless mirror radius. We have chosen parameters (30) so that FSR of the considered FP cavity was the same as for WGM cavities discussed above.

We chose the shape of the mirror similarly to the WGM cavity,

$$A(r) = x_0\exp\left(-\frac{r^2}{2R_cx_0}\right), \quad h_{1,2} = x_0 - A(r), \tag{31}$$

where $A(r)$ describes deviation from the mirror plane related to functions $h_{1,2}$ defined in (28). The particular shape is selected so that the curvature radius of the mirror stays the same as the optimal curvature of a spherical FP cavity with given dimensions. Our simulation shows that this condition corresponds to the lowest loss of the fundamental mode.

For the case of the FP cavity with identical mirrors we solved a discrete analog of Eqs. (29) numerically using the Hankel transform, resulting in considerable reduction of the evaluation time without accuracy loss (see [35] for details). Among all solutions we selected those with $|\xi|$ close to unity and found the corresponding eigenfunctions. The round-trip loss $\mathcal{L} = 1 - |\xi|^2$ allows finding finesse and the Q factor of the selected resonator modes: $Q = 2\pi L/(\lambda\mathcal{L})$.

The FP cavity with profile (31) has no bound modes if x_0 is small enough [Fig. 3(b)]. The fundamental mode becomes bound when x_0 reaches 7 μm. The higher-order modes are still unbound at this point. An increase of x_0 results in the increase of a Q factor of the fundamental mode while the Q factor of the other modes does not change. The first dipole mode becomes bound for $x_0 > 9$ μm, which is indicated by the increase of its Q factor. The maximum Q factor of the fundamental mode reaches 10^{10} at this point, and the ratio between Q factors of the fundamental and the first dipole modes reaches 1000.

D. Mirror shape optimization

We reported on simulations performed for a FP cavity that has a shape similar to that of the selected WGM cavity. This is done to confirm that both single-mode FP and WGM cavities have similar properties. We also found that Q factors of FP cavities depend on properties of shapes of their mirrors rather significantly, while single-mode WGM cavities are not very sensitive to their morphology. In this section we illustrate how changes in mirror morphology alter properties of the FP cavity modes.

We consider a FP cavity with identical mirrors having shape

$$A(r) = x_0e^{-\eta(1+\alpha\eta+\beta\eta^2)}, \quad \eta \equiv \frac{r^2}{2R_cx_0}, \tag{32}$$

where fitting parameters α and β are varied to get a combination of low diffraction loss of fundamental (main) mode (round-trip loss has to be $\mathcal{L} < 70$ ppm, which corresponds to quality factor $Q \geqslant 10^9$) and high loss of the other modes. The optimization is performed for each selected x_0 value. We found that the first dipole mode as well as the first axiosymmetric mode have the highest Q factors after the fundamental mode, so results for those modes only are presented (see Table I). The corresponding plots of Q factors for the fundamental, first axiosymmetric, and main dipole modes are shown in Fig. 7.

The optimized simulation shows that by choosing suitable fitting parameters one can realize the "single-mode" cavity (i.e., ratio between Q factors of main and next mode is larger

TABLE I. List of parameters α, β we used for different depths x_0 for profile (32); for depth $x_0 = 9$, 10 μm we put $\alpha = 0$, $\beta = 0$. The last column is the minimal ratio of diffraction losses of the main dipole mode (or first axiosymmetric mode) to losses of the main mode.

x_0 (μm)	α	β	Loss ratio
3	−0.1	0.3	150
4	0.2	0.425	110
5	0.2	0.25	390
6	0.12	0.175	570
7	0.116	0.05	690
8	0.0862	0.7	14 500
9, 10	0	0	

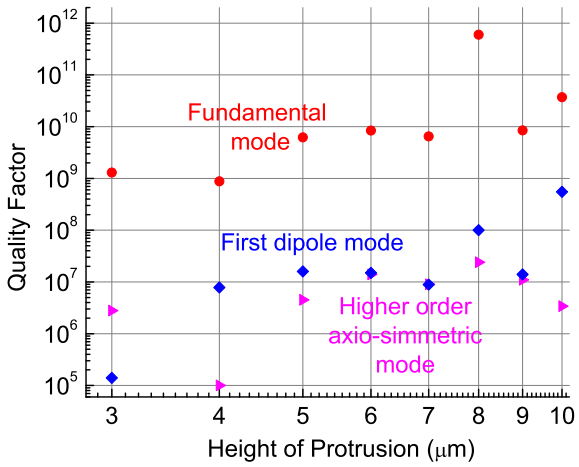

FIG. 7. (Color online) Dependence of the Q factors of the fundamental, first axisymmetric, and first dipole modes on the protrusion height FP cavity mirror profiles controlled by parameters α, β listed in Table I.

or about $\sim 10^3$) with relatively small shape deformation, $x_0 \geqslant 5\ \mu$m. It is important that the Q factor of the main mode is rather high and the diffraction-limited round-trip loss is exceptionally small, $\mathcal{L} \leqslant 7$ ppm, in contrast with more modest numbers predicted by earlier studies [20,21].

Moreover, we found combinations of fitting parameters that provide extremely small diffraction losses of the main mode, for example,

$$x_0 = 9.23\,\mu\text{m}, \quad \alpha = 0.156, \quad \beta = 0.606, \tag{33}$$

$$Q_{\text{main}} = 1.3 \times 10^{13}, \quad Q_{\text{dipole}} = 6.6 \times 10^{9}. \tag{34}$$

This corresponds to round-trip losses of the main mode $\mathcal{L} \sim 0.0042$ ppm. However, a small change in fitting parameters (α or β) by several percentage points results in a many times increase of diffraction losses of the main mode. It means that the mode becomes relatively unstable (difficult to realize in experiment) and we did not take this result into consideration.

IV. DISCUSSION

While the behavior of Q factors of a single-mode FP resonator is qualitatively similar to the behavior of the single-mode WGM cavity, there are certain differences. The range of x_0 values required for the single-mode operation is different. The curvature of the FP mirror is important, while the curvature of the WGM cavity protrusion is unimportant. The bound WGMs tend to have very high identical Q factors, while bound modes of a FP cavity have different Q factors even for an ideally matched spherical mirror. The protruded structure has much smaller dimensions than those of the single-mode WGM cavities, while the spatial change of the mirror profile has comparable dimensions with the mirror size in the case of the FP cavity. The mirror deformation does not look as the exaggerated view of Fig. 1 (see mirror profile in Fig. 6). Another difference between single-mode WGM and FP cavities is related to the fact that the WGM cavities are monolithic. The modes are localized in the nonlinear material and a change in intensity profile of light in the mode can modify its properties, including the Q factor.

While our study is purely theoretical in nature, it is important to discuss the possibility of fabrication of single-mode cavities. It may seem that the bound modes are sensitive to the residual disorder, unavoidable during any fabrication process. This is not the case with respect to the single-mode nature of the cavities. The bound fundamental modes are well localized and a small deterioration of the cavity morphology distorts them slightly. The unbound modes, on the other hand, are prone to changes in the quality of the surface of the cavity and its shape. Moreover, single-mode WGM cavities were observed experimentally [24,25], which confirms the feasibility of the concept. Earlier studies left questions about Q-factor limitation of the single-mode WGM cavity unanswered, and this paper fills the gap. Single-mode high-Q FP cavities have to be demonstrated.

It is important to note here that the Q factor of the single-mode FP resonator exceeds that of the FP resonator with ideally matched spherical mirrors of identical dimensions. Our simulation shows that this effect occurs because the bound mode has a super-Gaussian spatial profile. This mode is stable with respect to the boundary conditions. On the other hand, Q factors of single-mode WGM cavities do not exceed Q factors of multimode devices.

The single-mode WGM cavities considered here and discussed in Sec. II can be useful for generation of ultrashort pulses. It was shown that it is possible to retrieve sech-shaped optical pulses from a microresonator pumped with continuous wave light [36–41]. The duration of those pulses is given by the formula

$$\tau \approx 2\sqrt{\frac{-\beta_2}{\gamma F P_{in}}}, \tag{35}$$

where β_2 is GVD of the cavity modes ($\beta_2 < 0$ if the dispersion is anomalous), γ is the effective cubic nonlinearity of the cavity that depends on the cavity host material nonlinearity and mode volume, F is the cavity finesse, and P_{in} is the power of the continuous wave pump. Equation (35) predicts that the smaller $|\beta_2|$ is, the shorter the pulse can be.

In previous studies, the GVD of modes of a comparably large WGM cavity was measured experimentally and it was found that its actual value is orders of magnitude different than a theoretical number inferred from material properties and cavity mode structure [6]. It was concluded that the difference results from interaction among cavity modes. Mode interaction is eliminated from single-mode cavities and, hence, it should be possible to create a cavity with GVD not disturbed by mode interaction to generate ultrashort optical pulses.

Recently, the usefulness of single-mode cavities for Kerr frequency comb generation was demonstrated experimentally. It was shown that cavity morphology can be optimized to create a single-mode cavity with proper GVD and high Q factor to generate broad frequency combs with small pump power [42]. The Q factors of the experimentally demonstrated single-mode cavities reached 8×10^8, which is much better if compared with earlier experimental observations, but still slightly worse than the fundamental limit predicted in this work.

The single-mode FP cavities can be useful for improving laser gravitational wave detectors such as the Laser Interferometric Gravitational Wave Observatory (LIGO), because the dimensionless values (30c) are practically the same as those planned for LIGO:

$$\lambda = 1.064\ \mu\text{m}, \quad L = 4\ \text{km}, \tag{36a}$$

$$R_c = 2.076\ \text{km}, \quad r_m = 17\ \text{cm}. \tag{36b}$$

The analogy is important since usage of the single-mode FP cavity will prevent undesirable effects of parametric instability in laser gravitational wave detectors [14–18]. The parametric instability occurs as an excitation of the Stokes optical mode and elastic (mechanical) mode in the body of a cavity mirror if their frequencies, ω_s and ω_m, are related to the pump frequency ω_0 as $\omega_0 \simeq \omega_s + \omega_m$. The threshold of the effect is proportional to the product of quality factors of pump and Stokes modes. Stokes modes are usually high-order modes of a conventional FP cavity. The single-mode resonator does not support those modes and, hence, does not support parametric instability.

V. CONCLUSION

We have shown that it is possible to create high-Q single-mode WGM and FP cavities by optimizing their morphology. We found that the fundamental mode family of those cavities has quality factors comparable with conventional multimode cavities, while exceeding quality factors of the other modes by at least three orders of magnitude. Single-mode FP and WGM cavities perform in a similar way in spite of their different physical structure. The combination of the clean spectra and high-Q factors of the resonator is very promising for many applications, including generation of broadband Kerr frequency combs and creation of efficient gravitational wave detectors.

ACKNOWLEDGMENTS

Andrey B. Matsko, Fahmida Ferdous, and Lute Maleki acknowledge support from Defense Sciences Office of Defense Advanced Research Projects Agency under Contract No. W911QX-12-C-0067, as well as support from Air Force Office of Scientific Research under Contract No. FA9550-12-C-0068. A.A.D. and S.P.V. acknowledge support from the Russian Foundation for Basic Research (Grants No. 14-02-00399A and No. 13-02-92441 in the frame of program ASPERA) and National Science Foundation (Grant No. PHY-130586).

[1] G. D. Boyd and J. P. Gordon, Bell Syst. Tech. J. **40**, 489 (1961).
[2] A. A. Savchenkov, A. B. Matsko, D. Strekalov, V. S. Ilchenko, and L. Maleki, Electron. Lett. **41**, 495 (2005).
[3] G. S. Murugan, M. N. Petrovich, Y. Jung, J. S. Wilkinson, and M. N. Zervas, Opt. Express **19**, 20773 (2011).
[4] M. Ding, G. S. Murugan, G. Brambilla, and M. N. Zervas, Appl. Phys. Lett. **100**, 081108 (2012).
[5] M. Sargent III, M. O. Scully, and W. E. Lamb, Jr., *Laser Physics* (Addison-Wesley, Reading, MA, 1974).
[6] A. A. Savchenkov, A. B. Matsko, W. Liang, V. S. Ilchenko, D. Seidel, and L. Maleki, Opt. Express **20**, 27290 (2012).
[7] C. Bao, X. Xiao, and C. Yang, Phys. Rev. A **87**, 053844 (2013).
[8] T. Herr, V. Brasch, J. D. Jost, I. Mirgorodskiy, G. Lihachev, M. L. Gorodetsky, and T. J. Kippenberg, arXiv:1311.1716.
[9] I. S. Grudinin, L. Baumgartel, and N. Yu, Opt. Express **21**, 26929 (2013).
[10] Y. Liu, Y. Xuan, X. Xue, P.-H. Wang, A. J. Metcalf, S. Chen, M. Qi, and A. M. Weiner, arXiv:1402.5686.
[11] Y. Liu, Y. Xuan, X. Xue, P.-H. Wang, S. Chen, A. J. Metcalf, J. Wang, D. E. Leaird, M. Qi, and A. M. Weiner, arXiv:1405.6225.
[12] X. Xue, Y. Xuan, Y. Liu, P.-H. Wang, S. Chen, J. Wang, D. E. Leaird, M. Qi, and A. M. Weiner, arXiv:1404.2865.
[13] S. Ramelow, A. Farsi, S. Clemmen, J. S. Levy, A. R. Johnson, Y. Okawachi, M. R. E. Lamont, M. Lipson, and A. L. Gaeta, Opt. Lett. **39**, 5134 (2014).
[14] V. B. Braginsky, S. E. Strigin, and S. P. Vyatchanin, Phys. Lett. A **287**, 331 (2001).
[15] V. B. Braginsky, S. E. Strigin, and S. P. Vyatchanin, Phys. Lett. A **305**, 111 (2002).
[16] C. Zhao, L. Ju, J. Degallaix, S. Gras, and D. G. Blair, Phys. Rev. Lett. **94**, 121102 (2005).
[17] S. P. Vyatchanin and S. E. Strigin, Phys.-Usp. **55**, 1115 (2012).
[18] L. Ju, C. Zhao, D. G. Blair, S. Gras, S. Susmithan, Q. Fang, and C. D. Blair, Class. Quantum Grav. **31**, 185003 (2014).
[19] C. Pare, L. Gagnon, and P. A. Belanger, Phys. Rev. A **46**, 4150 (1992).
[20] M. Kuznetsov, M. Stern, and J. Coppeta, Opt. Express **13**, 171 (2005).
[21] B. Tiffany and J. Leger, Opt. Express **15**, 13463 (2007).
[22] R. D. Richtmyer, J. Appl. Phys. **10**, 391 (1939).
[23] V. V. Datsyuk and I. A. Izmailov, Phys.-Usp. **44**, 1061 (2001).
[24] A. A. Savchenkov, I. S. Grudinin, A. B. Matsko, D. Strekalov, M. Mohageg, V. S. Ilchenko, and L. Maleki, Opt. Lett. **31**, 1313 (2006).
[25] I. S. Grudinin, A. B. Matsko, A. A. Savchenkov, D. Strekalov, V. S. Ilchenko, and L. Maleki, Opt. Commun. **265**, 33 (2006).
[26] D. A. Neamen, *Semiconductor Physics and Devices: Basic Principles* (McGraw-Hill, Boston, 2011).
[27] A. A. Savchenkov, A. B. Matsko, V. S. Ilchenko, and L. Maleki, Opt. Express **15**, 6768 (2007).
[28] M. Oxborrow, IEEE Tran. Microwave Theory Tech. **55**, 1209 (2007).
[29] M. Cheema and A. Kirk, Opt. Express **21**, 8724 (2013).
[30] A. B. Matsko, A. A. Savchenkov, D. Strekalov, and L. Maleki, Phys. Rev. Lett. **95**, 143904 (2005).
[31] A. A. Savchenkov, A. B. Matsko, I. Grudinin, E. A. Savchenkova, D. Strekalov, and L. Maleki, Opt. Express **14**, 2888 (2006).
[32] J. U. Nöckel, Opt. Express **15**, 5761 (2007).
[33] A. E. Siegman, *Lasers* (University Science Book, Mill Valley, CA, 1986).
[34] S. Solimeno, B. Crosignani, and P. DiPorto, *Guiding, Diffraction and Confinement of Optical Radiation* (Academic Press, San Diego, 1986).

[35] J. Y. Vinet and P. Hello, J. Mod. Phys. **40**, 1981 (1993).
[36] A. B. Matsko, A. A. Savchenkov, W. Liang, V. S. Ilchenko, D. Seidel, and L. Maleki, Opt. Lett. **36**, 2845 (2011).
[37] A. B. Matsko, A. A. Savchenkov, V. S. Ilchenko, D. Seidel, and L. Maleki, Phys. Rev. A **85**, 023830 (2012).
[38] S. Coen and M. Erkintalo, Opt. Lett. **38**, 1790 (2013).
[39] K. Saha, Y. Okawachi, B. Shim, J. S. Levy, R. Salem, A. R. Johnson, M. A. Foster, M. R. E. Lamont, M. Lipson, and A. L. Gaeta, Opt. Express **21**, 1335 (2013).
[40] A. B. Matsko and L. Maleki, Opt. Express **21**, 28862 (2013).
[41] T. Herr, V. Brasch, J. D. Jost, C. Y. Wang, N. M. Kondratiev, M. L. Gorodetsky, and T. J. Kippenberg, Nat. Photon. **8**, 145 (2013).
[42] I. S. Grudinin and N. Yu, arXiv:1406.2682.